Journal of Internet Services and Applications, 2026, 17:1, doi: 10.5753/jisa.2026.7109

Intelligent Range Prediction and Trip Planning System for Amazon Electric Boats

Tatianna Aviz [**Universidade Federal do Pará** | ***tatianna.aviz@itec.ufpa.br***]
John Sousa [**Universidade Federal do Pará** | ***john.sousa@itec.ufpa.br***]
Dailneide Ribeiro [**Universidade Federal do Pará** | ***dailneide.ribeiro@itec.ufpa.br***]
Marlon Matos [**Universidade Federal do Pará** | ***marlon.matos@itec.ufpa.br***]
Lucas Bastos [**Universidade Federal do Sul e Sudeste do Pará** | ***bastos.lucas@unifesspa.edu.br***]
Iago Medeiros [**Universidade Federal do Pará** | ***iagomedeiros@ufpa.br***]
Emannuel Loureiro [**Universidade Federal do Pará** | ***emannuel@ufpa.br***]
Denis Rosário [**Universidade Federal do Pará** | ***denis@ufpa.br***]
Andréia Antloga [**Norte Energia** | ***andreianascimento@norteenergiasa.com.br***]
Eduardo Cerqueira [**Universidade Federal do Pará** | ***cerqueira@ufpa.br***]

Technology Institute, Federal University of Pará, Av. Perimetral, s/n, Universitário, Belém, PA, 66000-000, Brazil.

Received: 04 December 2025 • **Accepted:** 14 April 2026 • **Published:** 20 July 2026

Abstract The transition to sustainable transportation is critical in the Amazon, where riverine routes are vital for mobility and commerce. The adoption of electric boats is hindered by limited charging infrastructure and unpredictable environmental conditions. To address this challenge, we present an integrated system that combines real-time sensor monitoring with machine learning-based range prediction to reduce operator range anxiety and enable intelligent trip planning. The system incorporates battery discharge modeling based on Peukert's Law and employs Gaussian Process Regression, which achieved superior performance ($R^2 = 0.957$, RMSE = 2.545) among evaluated methods through its balance of accuracy, computational efficiency, and uncertainty quantification. The system was validated on an electric boat operating on the Xingu River, Brazil, equipped with LiFePO4 batteries. The system provides boat operators with real-time dashboards displaying live navigation data, battery status, and reliable range estimates, significantly reducing operational uncertainty. This work demonstrates a practical solution for accurate range prediction in remote environments, advancing sustainable electric maritime mobility (green computing) in the Amazon, which can be applied to similar waterways worldwide.

Keywords: Electric boats, Range Prediction, Machine Learning, Gaussian Process Regression, Peukert's Law, Riverine Transportation, IoT, Sustainable Mobility, Green Computing, Amazon, LiFePO4 Batteries.

1 Introduction

The growing demand for environmentally friendly transportation solutions has significantly accelerated the adoption of electric vehicles in multiple sectors, driven by the urgency of addressing climate challenges Damian *et al*. [2022]. In this context, the concept of green computing becomes a central theme in the design of modern mobility and energy infrastructures, leading to the efficient use of computational and communication technologies to minimize environmental impact. Although electric propulsion systems have gained widespread acceptance in passenger vehicles, their implementation in maritime transportation presents distinct obstacles that have hindered broader adoption Kersey *et al*. [2022]. This is particularly evident in the Brazilian Amazon Basin, where riverine navigation is a critical pillar of regional mobility and commerce. In this context, the movement of cargo via waterways reached 20.3 million tons in Q3 2023, accounting for more than half of the inland-waterways of Brazil during that period, underscoring the importance of efficient and sustainable transportation in the region Malheiros [2023].

Despite this, inshore boats remain predominantly powered by diesel fuel due to technical and infrastructure challenges that complicate the transition from fossil fuels (*e.g.*, gasoline or natural gas) to technologies powered by electricity Lima *et al*. [2024] Hernández-Fontes *et al*. [2021]. The global market for electric boats is projected to grow from USD 7.96 billion in 2025 to USD 14.45 billion by 2030, reflecting a growing global interest in sustainable maritime solutions Intelligence [2025]. However, in the Amazon, the lack of adequate charging infrastructure, combined with the high energy demands and weight constraints of battery packs, significantly impedes the widespread adoption of electric boats Moon *et al*. [2024].

In remote waterways, these technical limitations are exacerbated by scarce charging infrastructure Simavari *et al*. [2025], intensifying range anxiety (*i.e.*, the fear of being stranded with insufficient energy to reach the intended destination) Oyediran *et al*. [2024]. This concern is particularly acute in the Amazon, where unpredictable factors such as fluctuating water currents, wind speeds, and varying load conditions make static range estimation unreliable Candelo-Beccera *et al*. [2023]. Consequently, precise real-time autonomy prediction combined with intelligent trip planning become paramount to mitigate operational risks, enabling operators to navigate and schedule charging stops with confidence Al Amerl *et al*.

[2021].

In response to these challenges, this article presents an intelligent range estimation and trip planning system specifically designed for the unique conditions of waterway transportation in the Amazon Basin. This work is part of an energy efficiency project in collaboration with Norte Energia S.A. to design and develop an electric boat, aiming to reduce the environmental impact of traditional boats powered by fossil fuels in the region. The proposed system considers the collection of real-time sensor data from the electric boat, allowing the continuous monitoring of key variables such as boat speed, motor current, and battery levels. The system also offers accurate predictions of the remaining range of the boat under varying operating conditions by integrating a battery discharge model informed by Peukert's Law. We validated the predictive model using experimental data collected from an electric boat operating on the Xingu River (a tributary of the Amazon River), ensuring high accuracy and adaptability to local conditions in the Amazon Rainforest region. The real-time nature of the system allows operators to make decisions about route planning and charging stops, thereby reducing the uncertainty and operational risks associated with electric boats.

Our evaluation results show that Gaussian Process Regression (GPR) achieved superior performance compared to the evaluated Machine Learning (ML) methods, with $R^2 = 0.957$ and Root Mean Squared Error (RMSE) of 2.545. Hence, GPR provides a balance between accuracy, computational efficiency, and uncertainty quantification, making it particularly suitable for range estimation in remote environments. By enhancing operator confidence in their boat's autonomy, the system represents a crucial step toward facilitating the broader adoption of electric propulsion, paving the way for more sustainable and efficient maritime mobility in the Amazon.

In addition, this article advances Urban Computing by demonstrating how data-driven mobility intelligence can be incorporated into non-traditional urban infrastructure, such as river transport systems. The proposed system extends the principles of Urban Computing to river mobility infrastructures, enabling real-time integration of heterogeneous data flows (onboard sensors, environmental data, navigation parameters, and battery telemetry), predictive analytics, and intelligent decision support. Hence, the proposed system supports citizen-oriented mobility services, increasing safety, reducing operational uncertainty, and enabling more reliable public transportation in remote communities. By expanding knowledge about the development of electric vessel fleets, the study broadens the scope of smart mobility research into regions where river transport plays a central role, thus contributing to the development of smart waterways.

The main contributions of this article are stated as follows: (i) the design and implementation of a real-time monitoring and trip-planning system that combines sensor data with ML-based range prediction, providing operators a practical tool to mitigate range anxiety in remote riverine environments; (ii) a comparative evaluation of multiple regression methods for maritime range estimation, demonstrating that GPR achieves superior performance; (iii) the integration of battery discharge modeling based on Peukert's Law as part of the feature engineering pipeline, enabling physics-informed predictions that account for the nonlinear relationship between discharge current and usable capacity in LiFePO4 batteries; and (iv) the validation of the entire system through a real-world prototype involving an electric boat operating on the Xingu River in the Brazilian Amazon Basin. In this sense, we demonstrate the practical viability of the system in a remote environment with intermittent connectivity and limited infrastructure, paving the way for the broader adoption of sustainable electric boats in the region and similar waterways worldwide.

The remainder of this article is organized as follows. Section 2 presents related work on electric boat research and range prediction systems. Section 3 details the system design, including the architecture and the range prediction methodology. Section 4 describes the implementation details, experimental setup, results, and validation of the approach. Finally, Section 5 concludes the article and discusses future work.

2 Related Works

This article divides the state of the art into two distinct types of work: (i) an infrastructure for monitoring Internet of Things(IoT)-based energy management systems; and (ii) a range and energy prediction model.

2.1 Infrastructure Monitoring and IoT-Based Energy Management

Several works have explored technological advances in IoT-based control systems for electric vessels. For maritime-specific applications, Al Amerl *et al*. [2021] proposed a real-time energy distribution strategy between fuel cells and batteries for electric boats, focusing on improving the efficiency of power flow and reducing hydrogen consumption. However, this work does not directly address the challenges of fully electric boats in complex riverine environments.

Zhou *et al*. [2024] proposed an IoT-based maritime management framework that integrates sensor data acquisition with edge-computing components for boat-level decision-making. Their architecture leveraged smart gateways to aggregate real-time data from multiple sources on board, facilitating adaptive power distribution and environmental monitoring. Although promising for structured maritime operations, this approach depends on stable connectivity and infrastructure, which limits its applicability in our environmental context.

Jung *et al*. [2023] introduced a distributed sensor system for maritime IoT networks, using edge devices and mesh-based communication to ensure robust data transmission between vessels. The system supported energy-efficient routing and context-sensitive responses to dynamic navigation conditions. However, this work assumes a dense network of interconnected vessels, which is rarely available in isolated riverine regions where boats often operate individually.

Lobato *et al*. [2022] implemented a scalable monitoring system for electric vehicle charging stations in the Amazon region. Their work emphasized the importance of scalability in IoT platforms to handle large volumes of data generated by numerous charging stations. The system is capable of receiving and processing data from up to 160 charging stations,

Table 1. Summary of Related Works

Related Work	Range	Monitoring	Task	Vehicle
Al Amerl *et al*. [2021]	✗	✓	Energy Distribution and Control	Hybrid Boat
Zhou *et al*. [2024]	✗	✓	IoT-based Maritime Framework	Maritime Boat
Jung *et al*. [2023]	✗	✓	Distributed Edge and Sensor Systems (maritime IoT Networks)	Maritime Boats
Lobato *et al*. [2022]	✗	✓	Recharge Monitoring (IoT-based Infrastructure in the Amazon)	Electric Land Vehicle
Martins and Rodrigues [2025]	✗	✓	Charging Infrastructure Monitoring	Electric Land Vehicle
Dos-Reis *et al*. [2024]	✗	✗	Energy Consumption Prediction	Electric Land Vehicle
Kistner *et al*. [2023]	✗	✗	Energy Management	Large Maritime Boats
Chen *et al*. [2022]	✗	✗	Load Profile Estimation	Large Maritime Boats
Zhao *et al*. [2020]	✓	✗	Range Prediction	Electric Land Vehicle
De Vera and Cruz [2022]	✓	✗	Range Prediction	Electric Boats
Our Work	✓	✓	**Range Prediction and Trip Planning**	**Electric River Boat**

enabling efficient monitoring and management. This research presents a valuable reference for our work, as it illustrates how IoT platforms can be leveraged to manage distributed infrastructure, such as charging stations for electric boats, in remote and challenging environments.

Martins and Rodrigues [2025] presented a dedicated review of monitoring architectures for electric-vehicle charging infrastructure, with a particular focus on real-time oversight, IoT sensor integration, edge-computing, and cloud services to enable predictive maintenance and adaptive user behavior control. They identified key inefficiencies in charging-station usage (for example, vehicles that remain connected beyond optimal charge levels) and proposed a novel monitoring framework that addresses the technical, operational, and behavioral dimensions of charging-station monitoring. However, their work is based mainly on electric land vehicles.

2.2 Range and Energy Prediction

Dos-Reis *et al*. [2024] introduced a Machine Learning (ML) model to predict energy consumption in electric vehicles, incorporating factors such as driving behavior. This work focuses on various aspects of energy management and range prediction for electric vehicles, with a growing interest in maritime applications. Although its methodology provided a personalized approach to energy prediction, it is primarily applicable to land vehicles, making it less relevant to the unique environmental challenges faced by electric boats operating on remote waterways. This gap highlights the need for models specifically calibrated for maritime conditions.

Kistner *et al*. [2023] investigated the feasibility of electric container ships, addressing energy management and range prediction in commercial maritime transport. Although their findings are relevant for large-scale boats, their application to smaller river transport remains limited.

Chen *et al*. [2022] developed a model to predict the load profile of vehicle data using data from an operating ferry boat. The accurate load profile allowed for a deeper understanding of the system's energy demand patterns. As a result, it was possible to optimize energy consumption in hybrid vessels and, consequently, improve the efficiency of the energy system. However, the authors did not analyze range prediction.

Zhao *et al*. [2020] introduced a blended ML model that combines Extreme Gradient Boosting (XGBoost) and LightGMB to predict the remaining range of electric vehicles. They also proposed a method to address the issue of unbalanced dataset distribution. However, the authors did not mention the specific electric vehicle used, and the driving data suggests that it refers to a land vehicle.

De Vera and Cruz [2022] presented a framework to estimate the remaining range of electric boats. The accurate estimation of the remaining travel range depends on the precise calculation (Extended Kalman Filter) of the remaining energy capacity of the batteries, referred to as the (State of Charge (SoC)). The data obtained from the estimate SoC was then applied to provide predictions of the range in real-time.

2.3 Concluding Remarks

Table 1 presents a comparative analysis of related work, revealing a significant gap in the existing literature that our system addresses. Prior research can be categorized into two distinct groups: the studies focused on monitoring infrastructure (including charging station management and energy distribution) without addressing range prediction; and the studies focused on range estimation (through energy consumption models) without real-time monitoring capabilities. While monitoring-focused works enable system oversight, they do not provide operators with actionable range predictions. Conversely, range-focused studies model energy consumption but lack the real-time data integration necessary for dynamic operational adaptation.

Our work bridges this gap by integrating both capabilities into a unified system, enabling real-time range estimation informed by live operational data to support proactive trip planning and charging decisions. Furthermore, distinct from previous studies that rely on simulations or public datasets from other regions, this work introduces and analyzes a novel dataset collected from the Poraquê I vessel. To the best of our knowledge, this is the first work that explored real-world telemetry from electric boats in the Xingu River (or Amazonian) context for autonomy prediction tasks.

The existing literature often overlooks the specific challenges of electric boats operating in the Amazon, where the absence of charging stations, fluctuating water currents, and high energy demands present significant barriers to electrification. In addition, range anxiety remains a major obstacle to consumer adoption. Although some researchers have focused on optimizing route planning in electric vehicles, few have integrated real-time autonomy prediction with dynamic route optimization for electric boats in environments with fluctuating variables such as water currents, weather, and battery health. This holistic approach, which combines accurate autonomy estimates with actionable route planning, remains largely unexplored in the context of river transport. Our work fills this gap by developing a comprehensive autonomy planning dashboard specifically designed for Amazon river transport. This work integrates real-time sensor data and physics-informed battery models, calibrated with experimental data from electric boats operating on the Xingu River. In doing so, it provides a practical solution to the operational challenges identified in prior research, paving the way for the broader adoption of electric boats in the region.

3 System Design

This section describes the architecture and implementation of the proposed intelligent range estimation and trip planning system for electric boats. It outlines the real deployment context, hardware and software components, and data-management architecture that enables continuous monitoring and predictive analytics. The system integrates onboard sensing, local preprocessing on embedded hardware, and cloud-based storage with web dashboard visualization. The predictive subsystem combines physical calibration derived from Peukert's law with ML-based range estimation, forming a unified system optimized for real-time operation under the environmental and connectivity constraints of the Amazon region.

3.1 Real Scenario at the Brazilian Amazon Basin

This work focuses on the implementation of the electric boat system on the Xingu River, a vital waterway in the Brazilian Amazon Basin, particularly around the Belo Monte Hydroelectric Power Plant (*i.e.*, the largest in the Amazon). The region is known for its unique environmental and operational challenges, which significantly influence the performance and range of electric boats. For instance, the Xingu River, like many rivers in the Amazon Rainforest region, experiences seasonal fluctuations in water levels, characterized by pronounced wet and dry seasons. These fluctuations not only affect water currents but also influence boat efficiency and fuel consumption. In addition, the tropical climate of the region introduces variability in wind speeds, further complicating the task of accurately predicting the range and energy needs of the boats.

Electric boats operating on the Xingu River are primarily tasked with transporting passengers, cargo, and supplies between key locations near the Belo Monte Hydroelectric Power Plant. These boats follow predetermined routes, but the lengths of these routes can vary depending on environmental conditions. Boats must be designed to handle both calm and turbulent waters, ensuring consistent performance regardless of these conditions.

3.2 Battery Management System (BMS)

The safety and efficient operation of the electric boat's propulsion and onboard systems fundamentally depend on a dedicated Battery Management System (BMS), which acts as the central intelligence for the energy storage of the boat. The BMS is responsible for ensuring operational safety, maximizing battery life, and optimizing performance under varying load conditions. Constant monitoring of key parameters, such as voltage, current, and temperature, plays a critical role in preventing dangerous situations, such as overcharging, deep discharge (for range anxiety) or thermal failure, thereby guaranteeing the system's reliability.

The battery bank consists of three TSWB-LYP300AHA-B $LiFePO_4$ cells connected in parallel, providing a total nominal capacity of 900 ampere-hour (Ah) at a system voltage of 3.2 Volts (V). The BMS is specifically designed to manage this parallel configuration, incorporating high-precision monitoring and protection circuitry to oversee the pack as a unified system while ensuring that each individual cell is carefully protected. To achieve this, the BMS continuously monitors the battery health and operational state with high fidelity. The voltage of each cell is tracked with a precision of ±5mV, which is essential to detect imbalances that could lead to performance degradation or failure. Furthermore, strategically placed temperature sensors within the battery pack ensure that the system maintains optimal performance within 0°C (32°F) to 45°C (113°F), while supporting operation across the wider range of -20°C (-4°F) to 60°C (140°F) under less demanding conditions.

Electric current measurement is another critical aspect, with a Hall effect sensor (*i.e.*, which detects the current generated by magnetic fields) on the main bus providing accurate data within the range of ±500A. This collected information is used for Coulomb counting, which estimates the State of Charge (SoC) by integrating current over time, referencing the total nominal capacity of 900 Ah in 3P. The SoC is periodically calibrated against the voltage characteristics of the battery, ensuring accuracy throughout the discharge cycle De Vera and Cruz [2022].

Beyond real-time monitoring, the BMS also tracks the long-term health of the battery by estimating its State of Health (SOH), which refers to the battery's aging condition compared to when it was new. This is done by comparing the actual capacity of the battery with its nominal cell capacity of 300 Ah and monitoring the increase in internal resistance over time. Any significant changes in these metrics trigger an alert, enabling proactive maintenance before performance degradation impacts the boat's operation. To ensure optimal performance, the BMS also employs a passive resistive balancing system to manage voltage imbalances in the series-connected cells. When the voltage difference between two cells exceeds 20 mV, the system is activated to balance the cells, ensuring uniform voltage distribution and maximizing the usable capacity of the battery.

The BMS is equipped with a range of protective mechanisms to safeguard both the battery and the operation of the boat. Overvoltage protection halts charging if any cell voltage exceeds 3.65 V, while undervoltage protection disconnects the discharge circuit if any cell drops below 2.5 V. Overcurrent protection ensures that both charge and discharge currents remain within safety limits, while short circuit protection triggers an immediate system disconnection upon detection. Furthermore, the BMS includes overtemperature protection, which disconnects the battery if the pack temperature exceeds 45°C (113°F), preventing the risk of thermal runaway. These protection mechanisms are implemented through hardware circuits that physically isolate the battery from the system, ensuring that the boat remains safe under all conditions. For seamless integration with the boat's control systems (*i.e.*, the Raspberry Pi), the BMS communicates real-time data, including individual cell voltages, temperatures, and fault alerts, via a CAN bus interface.

3.3 System Architecture

Figure 1 provides an overview of the data collection and monitoring architecture that represents the entire data lifecycle, illustrating how real-time data flows from the electric boat to the dashboard. The system considers two elements, namely the command center and the electric boat. In addition, we consider an architecture composed of three layers: i) sensing; ii) real-time processing located in the electric boat's cabin; iii) historical processing located in the cloud, far from the electric boat's current location. This comprehensive diagram sets the stage for understanding how the real-time monitoring system integrates with prediction methods, bridging the gap between data collection, range prediction, and user interaction.

At the Sensing Layer, different sensors of the electric boat provide sensing data, which are sent to the Raspberry Pi (*i.e.*, a microprocessor-based single-board computer that acts as a central controller) through a Controller Area Network (CAN) bus transmission. For instance, the boat considers the real-time collection of trip record time, motor speed, motor temperature, controller temperature, and BMS-related information (*i.e.,* electric boat speed, voltage, current, and the desired motor operation mode (Economical, Normal, or Sport mode) defined by the boat operator).

The real-time processing layer is deployed on the Raspberry Pi in the electric boat cabin, which includes four modules: Data Collection, Real-time monitoring, Range prediction, and Message Queueing Telemetry Transport (MQTT) Publisher. Specifically, the Data Collection module receives the sensing data and stores it on the local database (*i.e.*, SQLite) to feed the real-time monitoring dashboard, the range prediction module, and the MQTT Publisher.

The real-time monitoring module (located inside the electric boat) exhibits the collected data in real-time on a dashboard to the user, allowing for continuous monitoring of key variables, such as boat speed and BMS information. This dashboard is displayed on a simple tablet screen to provide data visualization, which connects to the Raspberry Pi (performing all processing inside the boat) via a Bluetooth connection to consume data from the real-time monitoring module.

The range prediction module offers an accurate prediction of the remaining range of the boat. Finally, the MQTT Publisher module sends the real-time monitoring and range prediction data to the historical processing layer. It is important to mention that communication between the electric boat and the Command Center is challenging, as the boat experiences intermittent connectivity.

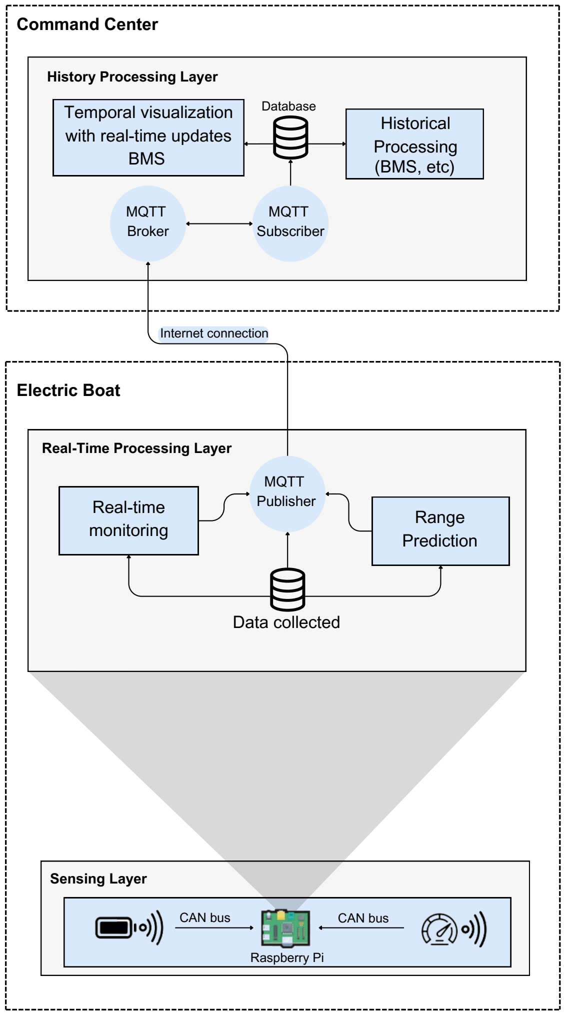

Figure 1. Data Collection and Monitoring Architecture Diagram

Finally, the historical processing layer works as an MQTT subscriber, receiving real-time updates through persistent connections to the broker. In this sense, the MQTT subscriber receives the uploaded information and stores it in the main database (*i.e.*, MongoDB). The database provides information for a comprehensive browsing history of past trips and also enables the temporal visualization of the current trip with real-time updates, using ML algorithms to determine the best trip planning approach accurately. Hence, this architecture allows the monitoring system to subscribe data from the electric boat, providing flexibility for different operational monitoring requirements. From a governance perspective, this cloud-based historical processing layer enables long-term data analysis to support infrastructure planning, charging station location strategies, the development of citizen services,

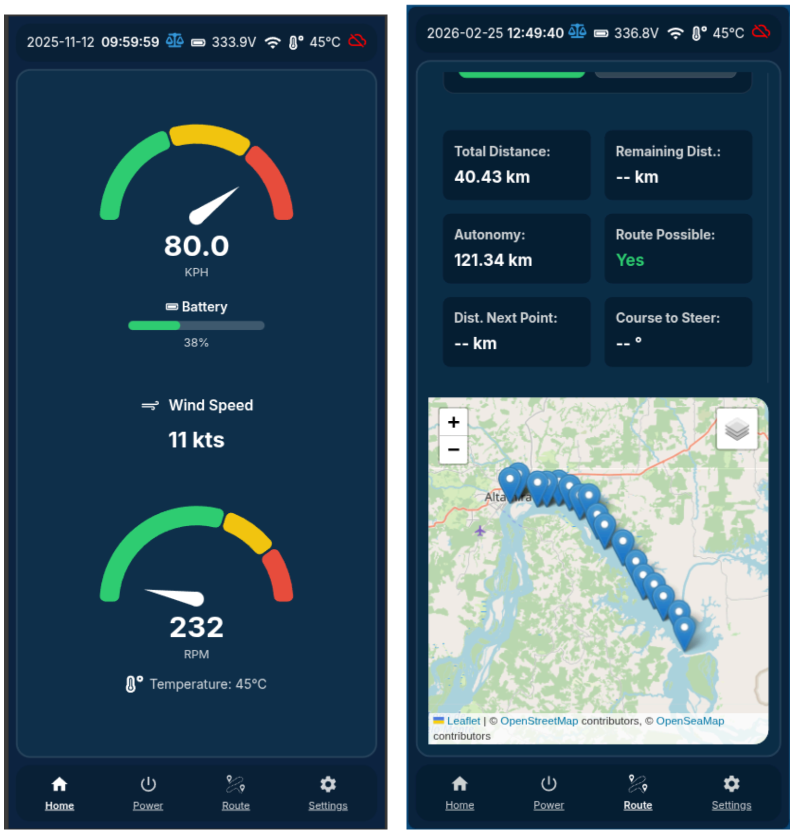

(a) Real-time Monitoring

(b) Visualization of route-planning with autonomy prediction

Figure 2. Operator Dashboard

and investments in sustainable transportation.

3.4 Real-time processing Layer

At the real-time processing layer, a Raspberry Pi unit serves as the MQTT publisher, collecting and preprocessing sensor data before transmission. This data is later forwarded to a cloud-based MQTT broker via an available internet connectivity, which acts as the central message hub.

3.4.1 Data Collection Module

Raw sensor data are first processed locally on the Raspberry Pi and then stored in a local SQLite database, which acts as a persistent buffer. This buffering mechanism ensures that no data is lost during periods of network outage when the boat is out of range of Wi-Fi or cellular signals.

3.4.2 Real-time Monitoring Module

The Real-time Monitoring Module consists of a dashboard developed in React.js, which provides monitoring information to the end-user (*i.e.*, the Boat Operator). Specifically, the dashboards display navigation data, route estimation, predictions, and primarily critical data based on the travel database. For instance, Figure 2(a) shows the Operator Dashboard with the data collection and monitoring process inside the electric boat. All important data provided by the electric motor is displayed in the Operator Dashboard in real-time. The Operator Dashboard uses four tabs: (i) Home, (ii) Power, (iii) Route, and (iv) Settings.

The first tab presents the most important data for the user in a simple and intuitive interface; the second tab shows the battery metrics, such as current charge, voltage, current, estimated duration, and battery health; the third tab comprises the travel planner and monitoring, providing an intuitive interface for the boat operator to select the desired route, plan the path that the boat will navigate, and monitor the travel; and finally, the fourth tab gives the user the option to select their desired configurations and manage the boat operator's profile.

The travel planner is responsible for setting the path that the electric boat will follow. The user enters the desired path, and the system calculates the viability of the proposed path, displaying the distance to travel, estimated battery consumption, and total travel time. For instance, Figure 2(b) shows the features mentioned for the route traveled by the Poraquê I electric boat. In addition to viewing data in real time on the Operator Dashboard, this information must be stored and monitored remotely for quick diagnostics of the boat's operation and failure prevention, with immediate support activated in case of problems.

The Travel Planner extends beyond passive visualization to provide active decision support. Upon destination selection, the system evaluates the energy feasibility. If the predicted consumption exceeds the safe range, the interface marks the route as "Impossible" and visually recommends the nearest charging station as a necessary intermediate waypoint. This mechanism transforms the dashboard into a proactive tool, effectively preventing operators from attempting unfeasible journeys based solely on intuition.

3.4.3 Range Prediction Module

Accurate prediction of battery autonomy in maritime environments requires precise modeling of discharge behavior, particularly under variable loads. Although traditional modeling approaches often rely on manufacturer-specified Peukert coefficients, these values must be appropriately selected based on the specific battery chemistry in use. Recent studies have revisited the Peukert effect in modern battery systems. For example, Rudy *et al*. [2023] demonstrated that all-solid-state cells follow a Peukert-type capacity discharge behavior, with the Peukert exponent varying across current densities. In addition, Galushkin *et al*. [2020] critically analyzed the classic Peukert equation and showed that its generalized form better describes the capacity behavior of rechargeable batteries over a wide range of currents. Moreover, Yazvinskaya *et al*. [2021] experimentally found that different discharge current intervals may require different Peukert-like modeling approaches. These findings supported the decision of this work to carefully consider the appropriate Peukert coefficient for the operational conditions.

In this work, Peukert's law was used not as a standalone predictive model but as a physical foundation to understand the nonlinear relationship between discharge current and usable capacity. This physical characterization serves two main purposes: (i) provides interpretable insights into the electrochemical behavior of the batteries used in the Poraquê I boat, and (ii) guides the extraction and calibration of features of the data-driven range estimation models presented in Section 4. The Peukert law, expressed in Equation 1, models the reduction in effective battery capacity as a function of the discharge current and forms the basis for this calibration. In this expression, T_1 and T_2 represent the discharge times at two different current levels (I_1 and I_2), and k is the Peukert coefficient.

$$k = \frac{\log(T_2) - \log(T_1)}{\log(I_1) - \log(I_2)} \tag{1}$$

For this study, the Poraquê I electric boat employs LiFePO4 (Lithium Iron Phosphate) battery modules (model TSWB-LYP300AHA-B). LiFePO4 batteries exhibit significantly better discharge rate efficiency compared to lead-acid batteries, with Peukert coefficients typically ranging from 1.01 to 1.05, indicating minimal capacity loss even under high discharge rates. This superior performance is due to LiFePO4's lower internal resistance and more stable electrochemical characteristics during high-current discharge. Given the manufacturer specifications and literature values for LiFePO4 chemistry, a Peukert coefficient of $k = 1.07$ was adopted for the range estimation system. This value represents a conservative estimate that accounts for the high-discharge and elevated-temperature conditions typical of Amazonian navigation, where battery performance may slightly deviate from ideal laboratory conditions. The adopted Peukert coefficient is used in Equation 2 and influences the final Equation 3.

This coefficient is integrated into the system as a reference parameter that informs the training and validation of the range prediction models. Specifically, it enables a more accurate interpretation of discharge behavior, specified at the BMS. Specifically, the remaining capacity CR_n of the battery at a given time (n) can be calculated from the current discharge rate (I) over a sampling interval Δt as demonstrated in Equation 2.

$$CR_{n+1} = CR_n - \frac{I^k \times \Delta t}{3600} \tag{2}$$

Where:

- CR_n is the remaining capacity at the current time step.
- I is the discharge current at that moment (in Amperes).
- k is the Peukert coefficient.
- Δt is the time interval between collected samples (in seconds).

Equation 2 calculates the remaining decrease in battery capacity based on current consumption over time, assuming a constant current draw during the interval. This enables the system to track the depletion of battery capacity throughout each trip.

In addition, the instantaneous range at any given time is determined by the remaining capacity and the current discharge rate. Equation 3 estimates how far the electric boat can travel before the battery is depleted.

$$\text{Range (h)} = \frac{CR_n}{I} \tag{3}$$

Where:

- Range (h) is the remaining range in hours.

Finally, the unit of the remaining range can be converted from time to distance in order to provide a more intuitive interpretation for the user. The remaining range expressed in hours can be converted to kilometers by multiplying the instantaneous range (in hours) by the instantaneous vehicle speed as expressed in Equation 4. Range (km) denotes the remaining range in kilometers, and Speed the instantaneous vehicle speed in kilometers per hour.

$$Range(km) = Range(h) \times Speed \tag{4}$$

These features provide valuable insights into the operational status of the boat, helping to estimate its autonomy in real-time, combating the range anxiety problem. The system uses a deployed ML method because it offers a more accurate range prediction, as it will train based on past trip records and the current trip status. A single solution without the ML method is inadequate, as it only provides the current status, and it is insufficient, since the data collected is highly volatile. This is because battery depletion is influenced by many internal factors (*e.g.*, battery discharge rate, SoC) and external factors (*e.g.*, wind speed, river current), where ML models can learn the range pattern more precisely.

3.4.4 MQTT Publisher Module

The deployment of electric boats in the Amazon region presents unique challenges for data transmission, particularly given the remote operational environment characterized by intermittent connectivity and limited bandwidth infrastructure. To address these constraints while maintaining reliable sensor data transmission from the boats to the cloud-based monitoring system, the MQTT protocol was selected as the foundation of the communication architecture. MQTT represents an optimal solution for these applications, as it operates efficiently in resource-constrained environments. This protocol offers several advantages over traditional HTTP-based communication protocols. The protocol's lightweight design, featuring minimal header overhead, significantly reduces bandwidth consumption, which is a critical consideration when relying on expensive satellite or cellular connections in remote riverine areas. Furthermore, MQTT's publish-subscribe messaging pattern provides inherent scalability and decoupling between data producers and consumers, enabling efficient distribution of sensor data to multiple endpoints without requiring publishers to maintain knowledge of subscriber identities.

This work implements MQTT's QoS levels based on data criticality to ensure data integrity across varying network conditions. Specifically, high-frequency and noncritical measurements, such as instantaneous speed readings, consider QoS 0 (at-most-once delivery), since this type of data accepts occasional packet loss in favor of reduced network overhead. On the other hand, critical operational data, including battery status and navigation parameters, employs QoS 1 (at least once delivered), guaranteeing message delivery through broker-mediated acknowledgment mechanisms. Finally, QoS 2 (exactly once delivery) remains reserved for configuration updates and control commands, though this represents a minimal portion of current system traffic. Regarding system security, the MQTT communications can be secured using TLS/SSL encryption to protect the telemetry payloads from interception, ensuring that vessel location and operational data remain private and secure from unauthorized access.

The system incorporates several mechanisms to maintain operational awareness during connectivity disruptions. Persistent sessions enable the broker to queue messages for temporarily disconnected clients (*i.e.*, the Command Center layer is the main client/subscriber because it receives the full MQTT transmission through the MQTT broker), ensuring that critical data is not lost during brief network outages. The Last Will and Testament (LWT) feature provides automatic notification of ungraceful disconnections, immediately alerting operators when the electric boat loses Internet connectivity. This distinction between intentional disconnect and communication failure enables the development of appropriate response protocols, which are particularly important when boats operate in areas with known coverage limitations.

The complete data transmission process follows a structured pipeline. Raw sensor measurements undergo preprocessing on the Raspberry Pi, including validation, unit conversion, and packaging into standardized JSON objects. These payloads are published on appropriate MQTT topics based on sensor type and boat identification. The cloud broker receives and immediately distributes messages to subscribed clients, primarily the React-based dashboard application. The dashboard utilizes an MQTT client library (HiveMQ) to maintain persistent connections and update the user interface in real time upon message receipt, eliminating the need for resource-intensive polling mechanisms. Figure 3 shows this MQTT-based communication architecture, which provides a robust foundation for real-time electric boat monitoring in challenging operational environments, such as the Amazon riverways.

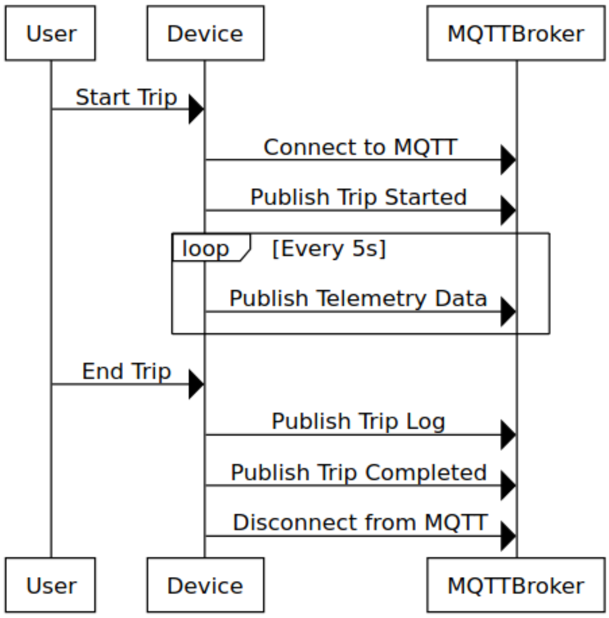

Figure 3. MQTT Diagram

3.5 Historical processing Layer

The historical processing Layer receives information from the Raspberry Pi using the MQTT Broker and subscriber when an Internet connection is available. Specifically, the received information is stored in the main database implemented with MongoDB, which provides content to the Browsing History Module and the Temporal Visualization Module.

3.5.1 Main Database

This work uses MongoDB as the main database located in the cloud since it is a well-suited database, especially for IoT implementations. MongoDB provides flexible cloud-native and multi-cloud support, time-series data handling, and good scalability without losing performance.

3.5.2 Browsing History and Real-time Monitoring Modules

The Command Center layer considers a Browsing History module developed to operate remotely, *i.e.*, located in the cloud. This module enables the analysis of the boat's travel history and controls recharging and routing.

The Command Center Dashboard, also developed with React and grouped by Vite, enables the ground support team to constantly monitor the main metrics displayed on the electric boat's operator panel. The internal structure was developed

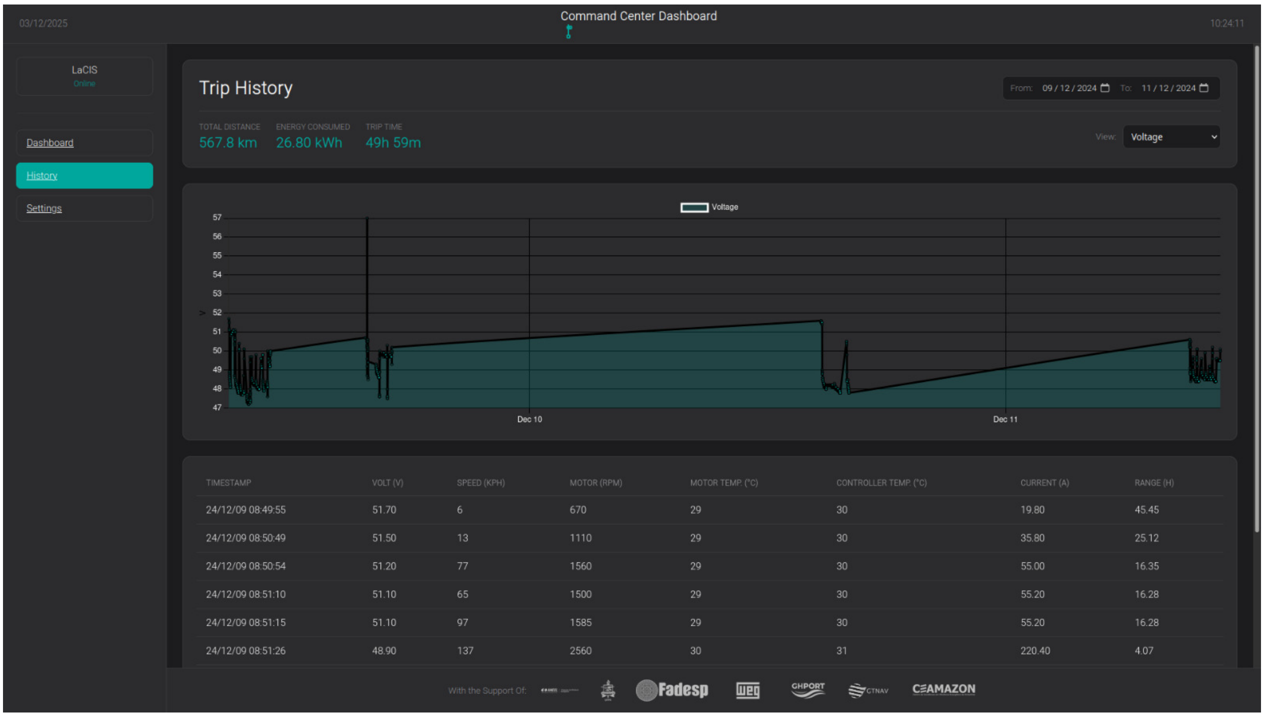

Figure 4. Command Center Dashboard

using the React.js Context API to facilitate the effective sharing of global states between components, thereby separating the logic of the visual interface from the logic of data collection.

Figure 4 shows the Command Center Dashboard, which is composed of a structure similar to that built into the Operator Dashboard. The Real-time Monitoring is exhibited in the Command Center Dashboard and serves as a helpful tool for the successful operation of the trip in the Amazon Basin. All important data provided by the electric-fueled motor is displayed in the Operator Dashboard in real-time. The dashboard comprises three tabs: (i) Main page, (ii) History, and (iii) Settings.

The first tab presents the most important data for the user in a simple and intuitive interface, providing a comprehensive overview of the electric boat's status through various graphs that display indicators such as battery status, electric boat speed, and electrical current consumption over time. Information about weather conditions, navigation direction, and location is also displayed. There is a side menu with tabs to display specific information for each monitored variable.

Figure 4 shows the complete trip history from the Browsing History Module) with detailed records, summary metrics such as speed, autonomy, energy consumption, and travel time; and allows data filtering by date ranges. In addition to the list of records, it is possible to select a variable and view a graph of its behavior during the selected period. Finally, the third tab offers the user the option to select the desired settings, such as language, alert limits for battery and motor temperature, and data update rates. All the electric boat's trips are recorded and uploaded constantly to a cloud-based system that stores them in a MongoDB database. This database stores the trip records to feed the range prediction system. The Command Center Dashboard is responsible for managing and training the range prediction system and stores all the electric boats' present and past trip status.

3.6 Complete Trip Monitoring: The Back-end Use Case

Figure 5 illustrates the complete dataflow pipeline, from raw data storage on board through preprocessing to remote cloud storage. The diagram shows the path of data from the sensors onboard, through local processing and buffering on the Raspberry Pi, transmission via MQTT to the cloud, and final storage in MongoDB for dashboard access.

Raw sensor data are first processed locally on the Raspberry Pi, where a preprocessing module filters out invalid sensor readings, such as zero values or out-of-range data, to ensure that only valid data is transmitted. This prevents erroneous range predictions and maintains the integrity of the system. The filtered data are then written to a local SQLite database, which acts as a persistent buffer. This buffering mechanism ensures that no data is lost during periods of network outage when the boat is out of range of Wi-Fi or cellular signals.

Whenever an Internet connection becomes available, the Raspberry Pi client initiates communication using the MQTT protocol. The client retrieves buffered records from the SQLite database and publishes them as JSON payloads to structured MQTT topics on a cloud-based broker *(i.e.*, MQTT Broker). Upon confirming successful publication (using QoS Level 1 for guaranteed delivery), Raspberry Pi removes the transmitted records from the local buffer to conserve storage space.

In case of failure in the cloud server or MQTT broker, the onboard Raspberry Pi continues to function autonomously, with local data storage and processing capabilities intact. The Operator Dashboard remains fully functional, allowing the

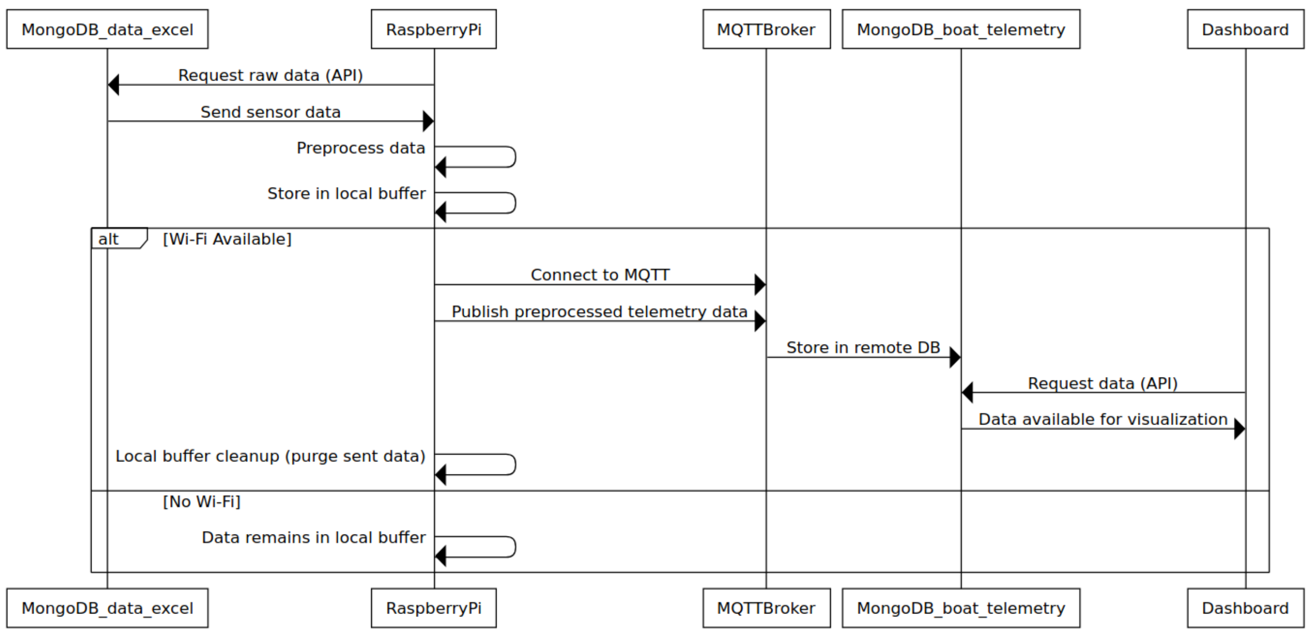

Figure 5. Data Collection and Dashboard Diagram

captain to monitor the system and make decisions based on locally processed data, ensuring safety is not compromised by shore-side infrastructure failures.

In addition, the onboard BMS continuously monitors the battery's health, with built-in protection mechanisms for overtemperature and overvoltage conditions. If any of these conditions are triggered, the system immediately sends an alert to the dashboard, notifying the operator of the physical fault and prompting corrective action.

To ensure operational reliability in the Amazonian environment, the system incorporates robustness mechanisms beyond network buffering. The local processing layer validates sensor data streams, flagging erratic readings (e.g., zero current during propulsion) to prevent erroneous predictions. Crucially, the system subscribes to BMS hardware alerts, triggering immediate dashboard alarms for critical faults such as cell overvoltage or overtemperature, prioritizing physical safety over navigation. Furthermore, the onboard dashboard functions independently of the cloud, ensuring navigation and range estimation remain available to the pilot even during total server isolation.

4 System Prototype

This section details the architecture and data pipeline of our intelligent range prediction system, which constitutes the core predictive module powering both the onboard and web-based dashboards. The system operates in two distinct phases: an initial model calibration phase, which utilizes historical operational data, followed by a real-time prediction phase deployed onboard the electric boat.

4.1 Dataset Description

This work is part of an energy-efficiency project in collaboration with Norte Energia S.A. to design and develop an electric boat, aiming to reduce the environmental impact of traditional fossil-fuel-powered boats in the region, which is currently under development and is still in its early stages. In this sense, the final real-world data collection has not yet been possible. Instead, we used data from a similar electric boat, named Poraquê I, which is eight meters long and can carry up to six passengers, operating near the Belo Monte Hydroelectric Power Plant on the Xingu River in the state of Pará, in northern Brazil [Norte Energia, 2023]. Figure 6 shows the Poraquê I, which refers to a typical South American electric fish (binomial nomenclature: Electrophorus electricus)

For the validation and telemetry of Poraquê I, data were collected from Poraquê I during test trips made by the boat transporting workers from Norte Energia S.A. The trips took place between December 9, 2024, and December 11, 2024, all following the same route of a 40 km between Altamira and Pimental, as shown in Figure 6. Specifically, the route traveled by the Poraquê I boat has two electric vehicle charging stations, located in Porto dos Areeiros in Altamira and in the Vessel Transposition System (STE) in Pimental (i.e., an auxiliary powerhouse downstream on the river). Besides not being collected for range estimation purposes, this dataset provides a reliable foundation for training the ML models used to predict the boat's range, contributing to a more accurate estimate of the boat's autonomy under development.

The full dataset consists of a total of 3,369 records, where Table 2 summarizes the primary variables relevant to estimating the remaining range. Specifically, the Record Time field stores the timestamp associated with each sample, enabling temporal synchronization between different data sources. Speed (in km/h) represents the translational speed of the electric boat and is a direct indicator of hydrodynamic load. Motor Speed (in Revolutions Per Minute, RPM) and Motor Temperature (in °C) describe the mechanical and thermal behavior of the propulsion subsystem, which are closely related to instantaneous power demand. The Controller Temperature

Figure 6. Belo Monte Hydroelectric Power Plant Complex on the left. Adapted from [Norte Energia, 2023]. Electric boat "Poraquê I" on the right [Mazzei, 2024].

(°C) provides additional context for thermal efficiency and system stress during operation. Voltage (V) and Current (A) correspond to the electrical input variables used to compute instantaneous power consumption and to estimate remaining energy capacity through Peukert-based discharge characterization. Speed Mode indicates the selected propulsion mode (Eco, Normal, or Sport), which reflects the operator's power-management strategy and affects both current draw and efficiency. The Eco mode is more energy-efficient, while Sport is the opposite. Auxiliary environmental parameters, such as wind speed and ambient temperature, are obtained from public meteorological APIs to capture external conditions that influence propulsion effort, but were not originally collected. Measurement of vessel load (*i.e.*, transported mass or passenger occupancy) was not available during data acquisition, as the data was collected only for validation and telemetry of Poraquê I. These data streams are continuously collected by an onboard sensor array connected to a Raspberry Pi microcontroller, which performs data aggregation, filtering, and real-time preprocessing before transmitting the information to the predictive system and dashboards.

Table 2. Variables in the generic electric boat dataset

Variable	Description	Unit
Record Time	Timestamp of data capture	—
Speed	Boat speed	km/h
Motor Speed	Motor rotational speed	rpm
Motor Temperature	Motor temperature	°C
Controller Temperature	Controller temperature	°C
Voltage	Motor voltage	V
Current	Motor current	A
Speed Mode	Motor operation mode (Eco, Normal, Sport)	—

4.2 Data Preprocessing

Data preprocessing follows acquisition and encompasses the removal of duplicates, handling of missing values (deletion or imputation), format conversions, and correction of inconsistent entries. This step ensures that both the real-time dashboard displays and the range predictions are based on reliable, high-quality input. To maintain the integrity of the dataset, a variety of preprocessing techniques were applied. The onboard microcontroller, a Raspberry Pi, handles data cleaning and filtering in real-time. For offline datasets, additional cleaning steps were applied to further refine the data.

One of the primary steps in the preprocessing was identifying the battery recharge events. These events are detected when there is a time gap of at least 12 hours between consecutive records, allowing the segmentation of the data for each day into separate trips. This step helps ensure that data associated with different travel events is not mixed, thereby preserving the uniqueness of each trip. Another step discards the records with zero values for critical parameters, such as revolutions per minute (RPM), the electric boat's speed, or the electric current; as these were interpreted as missing or invalid measurements. This step was necessary to eliminate records that could skew the analysis or lead to erroneous range predictions.

After applying these filters, the full dataset was reduced from 3,369 records to 2,671 records, ensuring that only relevant and valid data were used for analysis. The dataset is available[1] and it was prepared for utilization in this work. Once the data was cleaned, additional features were derived for use in the range prediction model. These included:

- Instantaneous Remaining Battery Capacity: The remaining battery capacity at any given time during the trip.
- Instantaneous Range: The estimated remaining range, displayed in hours or km.

Although the Instantaneous Remaining Battery Capacity was not directly recorded in the dataset, it was derived during the calibration phase from the integrated discharge current,

[1] `https://drive.google.com/drive/folders/1WTBliAgrfDwRwH4g2sRQFG_qOXwXH78H?usp=sharing`

as seen in Equation 2. The Instantaneous Range value was derived from the Equation 3.

For the real-time system, both values are computed onboard using the nominal capacity and measured discharge current. The relationship between current draw and effective capacity follows the Peukert-based discharge characterization established in Equation 1, ensuring that model input remains physically consistent with the underlying electrochemical behavior of the battery. The range prediction calculation utilizes MongoDB collections actively to determine the electric boat's actual situation, which is crucial for comprehensively assessing the electric boat's status and mitigating range anxiety.

4.3 Prediction Methods

Based on a comprehensive literature review, a wide variety of techniques used to estimate the range of electric vehicles were identified. Among these approaches, methods based on ML, artificial neural networks, and mathematical modeling stand out. In the development of this study, different techniques were implemented and analyzed. The methodologies evaluated are presented as follows.

4.3.1 Gaussian Process Regression (GPR)

The Gaussian process regression method is used as the prediction algorithm, which is a supervised ML method developed based on Bayesian theory and the Gaussian distribution. The prediction results were then integrated into the large-scale building energy monitoring system with the intention of comparing them with actual energy use in terms of the pre-defined criteria, including deviation values, percentage, and statistical analysis indicators Zeng *et al*. [2020].

4.3.2 Support Vector Regression (SVR)

Support Vector Regression (SVR) is an extension of the maximum margin principles of Support Vector Machines (SVM) for regression tasks. The method seeks a function that fits the data by minimizing the error within an acceptable margin ε, while controlling the complexity of the model through regularization of the weight vector. Only training points whose error exceeds this margin (called support vectors) influence the final form of the regression function. The optimization problem is convex and can employ kernel functions to map the data to high-dimensional feature spaces without the need for explicit computation, allowing nonlinear relationships to be captured with good generalization ability Smola and Schölkopf [2004]. This property makes SVR particularly useful in estimating the range of electric vehicles, as energy consumption depends on multiple interdependent and nonlinear factors. Recent studies have evaluated SVR-based models for both range prediction and EV energy consumption Pokharel *et al*. [2021], reporting better performance compared to other regression algorithms Ahmed *et al*. [2022].

4.3.3 Multilayer Perceptron (MLP)

The Multilayer Perceptron (MLP) is a feedforward artificial neural network composed of multiple fully-connected layers of neurons and is capable of modeling complex nonlinear mappings between input features and target outputs. In the electric vehicle domain, the MLP is used for predictive tasks such as energy consumption, emission estimation, or battery behavior modeling; for example, an MLP combined with a meta-heuristic algorithm improved CO_2 emission predictions for electric vehicles Saqr *et al*. [2025]. Its flexibility makes it a strong choice where data volume is moderate, and interpretability is a lower priority.

4.3.4 Extreme Gradient Boosting (XGBoost)

Extreme Gradient Boosting (XGBoost) is an ensemble technique based on a set of decision trees designed to optimize performance and generalization in prediction tasks. In practice, a single decision tree may not be robust enough to capture complex relationships between input variables. To overcome this limitation, XGBoost combines multiple sequentially trained trees, where each new tree is adjusted to minimize the residual error gradient of the model accumulated up to that point Chen and Guestrin [2016]. Thus, each subsequent tree seeks to correct the prediction errors of the previous trees, and the final prediction is obtained through a weighted sum of the individual outputs of the trees. XGBoost is one of the most widely used techniques for estimating the reach in VEs Zhao *et al*. [2020] Hosseini *et al*. [2024] due to its ability to capture complex interactions and handle heterogeneous data.

4.3.5 Random Forest (RF)

The Random Forest (RF) algorithm is an ensemble learning method that aggregates predictions of many decision trees, trained on random subsets of data and features, to produce robust regression or classification results. In electric vehicle studies, RF has been used to predict battery state of charge, driving range, or charging loads. For example, RF accurately estimated the SoC of the EV battery in a recent study Sulaiman and Mustaffa [2024]. Its robustness to overfitting and ability to handle mixed feature types make it well-suited for vehicle operational data, which often includes categorical, numerical, and sensor-derived inputs.

4.3.6 Gradient Boosted Regression Trees (GBRT)

Gradient Boosted Regression Trees (GBRT) represent an ensemble approach that sequentially builds regression trees to improve prediction accuracy. Each tree in the sequence focuses on correcting residual errors from previous trees, with the ensemble's final output combining individual tree contributions Friedman [2001]. GBRT's iterative refinement strategy enables effective modeling of complex variable interactions, making it suitable for energy consumption prediction in electric vehicles. The method's ability to quantify feature importance provides interpretative value for understanding which operational factors most influence the range estimation.

4.3.7 Linear Regression (LR)

Linear Regression (LR) is a classical statistical learning method that models the relationship between dependent and independent variables via a linear equation. Despite its simplicity, in electric vehicle research, it serves as a baseline model to estimate relationships such as vehicle speed, trip duration, and energy consumption; for example, a multiple linear regression model predicted the average energy demand of electric vehicles from kinematic parameters like average speed and number of stops Ahmed *et al*. [2022]. Because of its interpretability and low computational cost, LR is often used as a benchmark for comparisons with more complex models.

4.3.8 Time Series Forest (TSF)

Time Series Forest (TSF) is an ensemble method specifically designed for temporal data analysis, constructing multiple decision trees using features derived from time-series subsequences Deng *et al*. [2013]. The method extracts statistical features (mean, standard deviation, slope) from random intervals within the series and aggregates predictions across trees to produce robust estimates. TSF's computational efficiency and ability to identify discriminative temporal patterns make it applicable to capturing energy consumption dynamics during electric vessel navigation.

4.3.9 Long Short-Term Memory (LSTM)

The Long Short-Term Memory (LSTM) network is a type of recurrent neural network designed to capture long-term temporal dependencies in sequential data, using gating mechanisms to avoid vanishing gradients. In the electric vehicle context, LSTM is applied to tasks such as predicting battery failure or degradation (*e.g.*, voltage failure) using vehicle time-series operational data. Its ability to process sequential sensor data (*e.g.*, charge/discharge cycles, driving behavior over time) makes it powerful for predictive maintenance and dynamic energy management Li *et al*. [2023].

4.4 Range Prediction Test

The raw dataset used to train the range-prediction methods included variables for navigation, propulsion, and battery, as well as derived features obtained from Peukert-based feature engineering. Following standard ML practices, the dataset was partitioned into training sets (80%) and test sets (20%) using temporal splitting to prevent data leakage. Model tuning was then performed using grid search, which systematically evaluates combinations of hyperparameters through a 5-fold cross-validation procedure executed in parallel and optimized using MAE.

All ML models were implemented in Python 3.9 using established libraries: scikit-learn 1.2.0 for traditional ML methods (GPR, SVR, RF, GBRT, MLP, LR, TSF), XGBoost 1.6.0, and TensorFlow 2.8 for LSTM. Training was performed on a workstation equipped with an Intel Core i9-13900K processor and 128GB RAM. Input features included boat speed (km/h), motor current (A), battery voltage (V), and derived Peukert-based features (remaining capacity in Ah), among others, exemplified in the cleaned dataset. All features were standardized using z-score normalization ($x_{scaled} = (x - \mu)/\sigma$) to ensure consistent scaling across different measurement units.

Hyperparameter optimization was conducted using appropriate validation strategies for each model type. Gaussian Process Regression employed a Matern kernel ($\nu = 1.5$) with automatic relevance determination, optimized via marginal likelihood maximization. Support Vector Regression utilized grid search to determine optimal regularization (C=10) and margin width ($\epsilon = 0.01$). Ensemble methods (XGBoost, Random Forest, GBRT) employed early stopping and out-of-bag validation to prevent overfitting. Neural networks (MLP, LSTM) used training/validation splits with early stopping based on validation loss. LR does not have important hyperparameters to mention.

Specifically, MAE and RMSE are expressed in hours (i.e., the same as the range), representing the average and root-mean-square prediction errors in remaining operational time, respectively. The R^2 coefficient is dimensionless (ranging from 0 to 1) and indicates the proportion of variance explained by the model. MAPE is expressed as a percentage and represents the average relative prediction error. For operational context, an MAE of 0.5 hours corresponds to predictions accurate to within approximately 30 minutes, which is suitable for trip planning in riverine navigation, where typical journey durations range from 2 to 8 hours.

Figure 7 presents the RMSE comparison across all evaluated models, measured in hours of remaining operational time. GPR and SVR achieved the lowest RMSE values at 2.545 and 2.546 hours, respectively, indicating highly consistent predictions with minimal large errors. The MLP showed moderate performance with an RMSE of 3.018 hours, while ensemble methods displayed varied performance: XGBoost (3.364 hours), Random Forest (3.523 hours), and LSTM (4.122 hours). TSF recorded an RMSE of 4.499 hours, and GBRT exhibited the highest error at 5.055 hours among competitive methods. Linear Regression performed poorly with an RMSE of 6.396 hours, confirming that simple linear models are inadequate for capturing the nonlinear discharge dynamics. The near-identical RMSE values between GPR and SVR suggest both methods effectively model the underlying energy consumption patterns, though their approaches differ fundamentally—GPR through probabilistic inference and SVR through margin-based optimization.

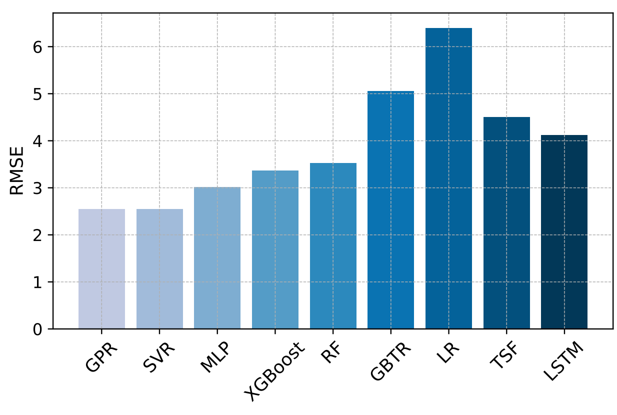

Figure 7. RMSE

Figure 8 illustrates the proportion of variance explained by each model, with values closer to 1.0 indicating a better fit. GPR and SVR both achieved the highest R^2 of 0.957, demonstrating their ability to explain approximately 96% of the variance in remaining operational time. The MLP followed closely with an R^2 of 0.939, showing that neural approaches can effectively capture complex patterns when properly configured. Ensemble methods showed moderate performance: XGBoost (0.924), Random Forest (0.917), and GBRT (0.829), with GBRT's lower value suggesting potential underfitting or sensitivity to hyperparameter choices. Notably, Linear Regression achieved an R^2 of 0.726, indicating it captures basic trends but misses critical nonlinear interactions. The temporal methods (LSTM at 0.590 and TSF at 0.512) exhibited lower R^2 values despite their design for sequential data, possibly due to the relatively short temporal sequences in individual trip segments or the dominance of instantaneous discharge characteristics over historical patterns in determining remaining range.

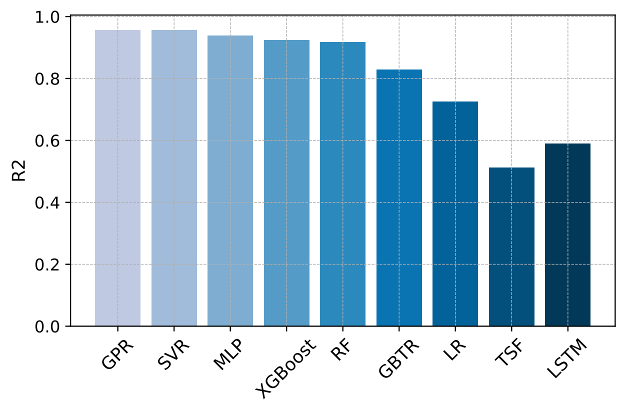

Figure 8. R^2

Figure 9 displays the average absolute prediction error in hours, providing an intuitive measure of typical prediction accuracy. The LSTM model achieved the lowest MAE of 0.400 hours, followed by SVR at 0.505 hours and GPR at 0.561 hours. These values indicate that top-performing models typically predict remaining operational time within a half-hour window, which is operationally acceptable for trip planning in riverine navigation. XGBoost, Random Forest, and TSF showed moderate errors, while GBRT (1.014 hours) and MLP (1.100 hours) exhibited larger average deviations. Linear Regression's MAE of 2.805 hours demonstrates its fundamental inadequacy for this application. While LSTM achieved the best MAE, this metric alone does not account for computational cost, uncertainty quantification, or worst-case performance—factors critical for embedded deployment in safety-critical applications.

Figure 10 presents the relative prediction errors as percentages, providing a scale-independent performance comparison. LSTM demonstrated exceptional relative accuracy at 1.715%, indicating predictions within 2% of actual values on average. SVR (6.787%) and TSF (7.856%) followed with strong performance, while GPR achieved 8.307%, which is reasonable for practical maritime applications. XGBoost (10.997%), Random Forest (14.009%), MLP (18.800%), and GBRT (19.622%) showed progressively higher relative errors. Linear Regression's MAPE of 49.757% confirms its unsuitability for this nonlinear prediction task. The low MAPE values across top-tier methods (below 10%) reflect both the quality of the dataset and the appropriateness of selected input features (velocity, current, voltage, Peukert-derived capacity). Notably, while LSTM achieved the best MAPE, the difference between LSTM (1.715%) and GPR (8.307%) must be weighed against computational requirements and uncertainty quantification capabilities in the context of real-time embedded deployment.

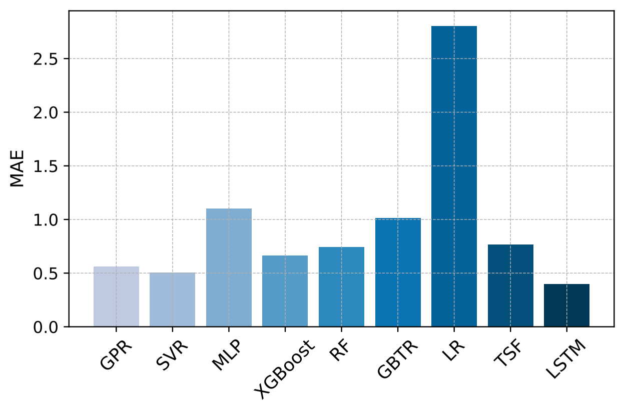

Figure 9. MAE

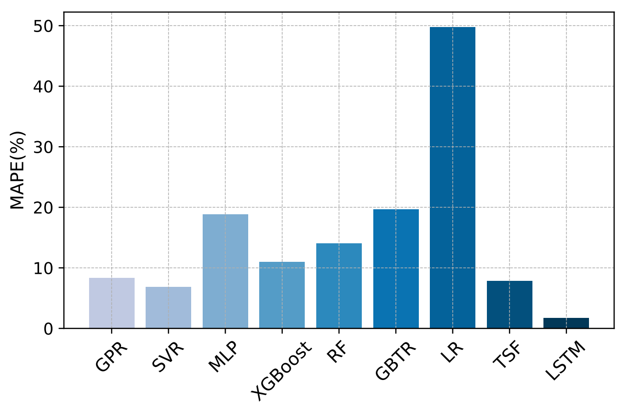

Figure 10. MAPE

A key and perhaps unexpected finding emerged from the model evaluation. Although the Long Short-Term Memory (LSTM) model yielded superior raw accuracy metrics (MAPE of 1.715%, as seen in Figure 10), it carries a significant computational overhead that is unsuitable for real-time inference on the low-power embedded hardware of the electric boat. More critically, GPR provides inherent uncertainty quantification, a feature deemed essential for this safety-critical application. In a system designed to mitigate range anxiety, the operator's ability to see a confidence interval for the range (rather than a single-point estimate) is more valuable than a marginal gain in raw accuracy. This practical trade-off itself is a central finding of our work. The Peukert-based feature engineering remains incorporated as a physical reference that informs this method's feature derivation, ensuring that its predictions remain consistent with the battery's actual electrochemical behavior.

Given its superior balance of precision, computational efficiency, and uncertainty quantification, the GPR method was selected for integration into the dashboard's range prediction module as the final ML model. Table 3 summarizes the complete performance metrics for all evaluated methods.

This choice ensures reliable range estimation under various operational scenarios and directly supports the system's objective of reducing range anxiety for electric boat operators navigating in the Amazon region.

Table 3. Evaluation of Methods in the Test Set

Model	MAE	RMSE	R^2	MAPE
GPR	0.561	**2.545**	**0.957**	8.307%
SVR	0.505	2.546	**0.957**	6.787%
MLP	1.100	3.018	0.939	18.800%
XGBoost	0.666	3.364	0.924	10.997%
RF	0.745	3.523	0.917	14.009%
GBTR	1.014	5.055	0.829	19.622%
Linear Regression	2.805	6.396	0.726	49.757%
TSF	0.767	4.499	0.512	7.856%
LSTM	**0.400**	4.122	0.590	**1.715%**

4.5 Dashboard System Validation Test

This work conceptually validated the trip-planning functionality of the dashboard through a series of simulated route scenarios of varying complexity. Although full-scale execution tests were not possible within the project timeline, the system consistently demonstrated the ability to generate viable navigation paths with integrated charging recommendations. In cases where the available battery level was insufficient for a direct route, the algorithm correctly suggested alternative itineraries that incorporated intermediate charging stops, thus mitigating the risk of range-related interruptions. Preliminary evaluations conducted during Poraquê I's operational trips confirmed that the range-prediction module on the dashboard aligned closely with real-world consumption trends, contributing to a measurable reduction in operator uncertainty during navigation on the Xingu River.

The results demonstrate the system's robust data handling during network disruptions. During controlled testing, this test simulated a 5-minute Wi-Fi outage while the electric boat continued to operate, a scenario that is very possible in the Xingu River and other Amazon rivers. The SQLite local buffer (located at the Raspberry Pi) successfully stored all 150 generated data points without loss, with automatic synchronization to the MongoDB database in the cloud (located at the Command Center Dashboard) occurring within 2 seconds after network restoration. This capability proved crucial during actual operations on the Xingu River, where cellular coverage is intermittent, ensuring continuous data availability for both real-time monitoring and historical analysis. The system successfully handled simulated sensor failures by filtering out invalid data during local processing on the Raspberry Pi. Invalid readings, such as zero values or out-of-range data, were excluded from transmission, ensuring the system continued to function without erroneous range predictions.

The system's local autonomy was thoroughly tested during network failures. In scenarios where the cloud server or MQTT broker was unavailable, the Raspberry Pi continued to operate independently, storing telemetry data locally and ensuring uninterrupted monitoring. The Operator Dashboard remained fully functional, providing real-time data display and route planning without reliance on cloud infrastructure.

To evaluate the scalability of the system, this work conducted stress tests by simulating various electric boats operating concurrently. The MQTT broker efficiently managed data streams from five simultaneous boat connections, ensuring consistent message delivery without loss at QoS Level 1. The MongoDB database maintained consistent performance with 50,000 historical records, with the query response times under 10 seconds for complex historical analyses (when analyzing the full dataset at the Command Center Dashboard). This dashboard supported three simultaneous operator sessions without performance degradation, demonstrating the architecture's readiness for fleet-scale deployment.

The BMS integration was validated during the testing, ensuring that any critical battery conditions (such as overtemperature or overvoltage) were detected. Alerts were successfully triggered on the dashboard, notifying the operator and providing timely warnings to prevent potential damage to the battery. The system's resilience was tested through intentional failure scenarios. During a simulated Raspberry Pi hardware failure and subsequent reboot, the system automatically reestablished MQTT connections and resumed data transmission in 1 minute on average. The Last Will and Testament feature from MQTT immediately alerted operators to the disconnection, enabling a prompt response. Data integrity was maintained throughout, with zero records lost during the recovery process. These features provide critical operational assurance in the remote Amazon environment, where technical support may be hours away.

Table 4 summarizes the key performance metrics obtained during system validation. The dashboard's real-time data display maintained an average latency of 1.2 seconds from sensor measurement to operator screen, well within acceptable limits for navigation decision-making. The route planning algorithm successfully processed 142 of the 145 test routes, with three failures occurring only in extreme scenarios involving simultaneous unavailability of multiple charging stations.

It is important to clarify that, in the context of Amazonian river navigation, the route planning function does not perform spatial pathfinding between alternative trajectories, as navigable channels are typically fixed. Instead, the system evaluates the energy feasibility of the planned route given the current battery condition and the availability of charging stations along the way. When the battery level is insufficient for a direct trip, the algorithm identifies the nearest intermediate charging stop on the same route. The 145 simulated scenarios tested varied battery conditions and charging station availability to validate this decision logic.

4.6 Sensitivity Analysis

In this section, we introduce a sensitivity analysis to evaluate the impact of the Peukert coefficient on the battery discharge performance of different ML models. Specifically, we considered two coefficients (*i.e.*, $k = 1.10$ and $k = 1.15$), since the Peukert coefficient is directly related to the remaining battery capacity and autonomy (as described in Equation 2). Figure 11 shows the remaining battery capacity over time, expressed

Table 4. Measured system performance metrics during validation

Metric	Type Test	Value	Test Conditions
Network outage tolerance	Network	5 min	Zero data loss during controlled Wi-Fi outage; automatic resynchronization within 2 s after recovery
Multi-user support	Stress	5 operators	Concurrent dashboard sessions without noticeable performance degradation
Historical data query	Stress	<10 s	Query time for 50,000+ record database under complex search conditions
System recovery time	Network	1 min	Automatic reconnection and data-flow restoration after simulated hardware reboot
Data transmission latency	Network	1.2 s	Average end-to-end delay from sensor measurement to dashboard display
System accuracy	Processing	97.9%	142 of 145 successful experiments

in minutes, for different coefficient values, which is limited to the first day of operation. It can be observed that as the value of k increases, the battery discharges more rapidly, leading to a quicker decline in the available capacity. The curves are initially close, as all the scenarios start from the same nominal capacity. However, the difference increases progressively due to the cumulative, nonlinear nature of Peukert's law. By the end of the trip, for $k = 1.15$ the capacity falls below 100 Ah, whereas for $k = 1.07$ it remains close to 400 Ah. This behavior demonstrates that higher Peukert coefficients correspond to a stronger dependence of the effective battery capacity on the discharge profile, significantly reducing the predicted autonomy.

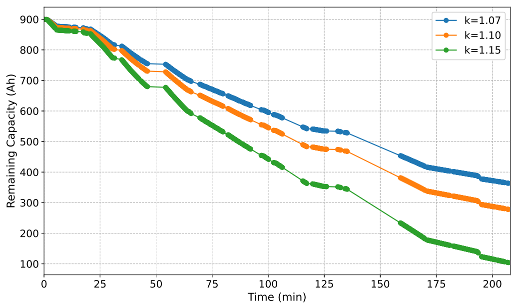

Figure 11. Remaining Capacity over Time

Figure 12 shows the R^2 results for the evaluated ML models, where we selected only the three ML models with the best overall performance for detailed analysis, *i.e.*, SVR, GPR, and RF. For $k = 1.10$, GPR exhibited a noticeable reduction with R^2 of 0.684, whereas SVR and RF maintained higher stability with 0.930 and 0.869, respectively. At $k = 1.15$, performance improved again, with SVR achieving 0.984, GPR 0.972, and RF 0.947. Compared to the original configuration ($k = 1.07$), these results indicate that coefficient variation mainly affects GPR, while SVR preserves greater stability.

Figures 13 and 14 present the MAE and RMSE results, respectively, both expressed in hours. While the baseline results were previously discussed, increasing the coefficient reduces the MAE for SVR, reaching 0.326 hours at $k = 1.15$. In contrast, GPR and RF exhibit greater fluctuations, indicating higher susceptibility to variations in the discharge modeling parameter. A similar trend is observed for RMSE:

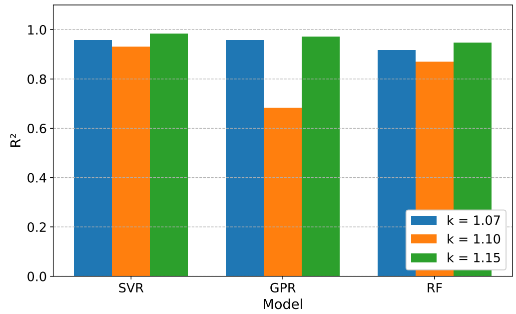

Figure 12. R^2

at $k = 1.15$, SVR achieves the lowest value (1.604 hours), whereas GPR and RF reach 2.113 hours and 2.791 hours, respectively. Since RMSE penalizes larger deviations more strongly, these results confirm that SVR maintains lower large-error magnitudes as the nonlinearity of the discharge process increases.

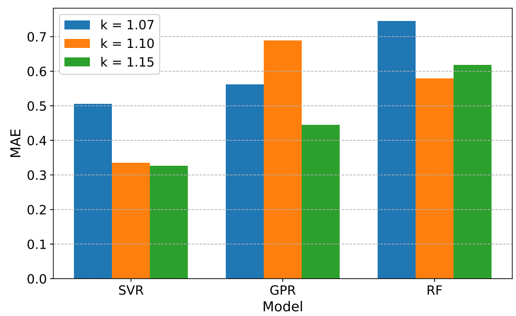

Figure 13. MAE

Finally, Figure 15 indicates that the relative errors also vary with the Peukert coefficient. Although SVR achieves its lowest percentage error at $k = 1.10$ (3.933%), RF reaches 16.759% at $k = 1.15$, indicating greater relative dispersion under stronger nonlinear discharge effects. Overall, SVR demonstrates the most consistent performance across all evaluated metrics. Despite the influence of coefficient variation on prediction accuracy, the original value $k = 1.07$ remains technically justified, as it aligns with manufacturer specifications and is commonly reported for lithium-based battery systems.

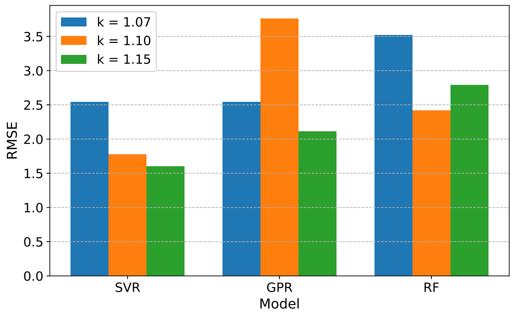

Figure 14. RMSE

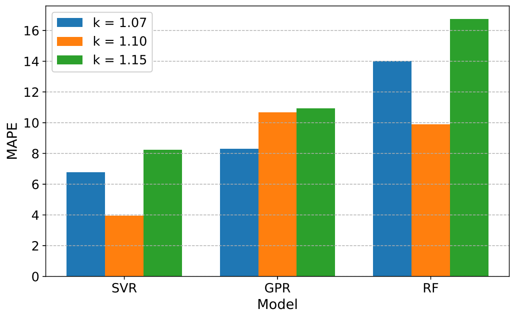

Figure 15. MAPE

4.7 General Discussion and Open Issues

The battery-physics-informed ML system deployed strikes a practical balance between prediction accuracy, computational efficiency, and operational safety. This work provides reliable range guidance that meaningfully reduces operator range anxiety (one of the main barriers to electric boat adoption in remote regions). The conservative bias observed at high discharge currents (a systematic $\approx 6\%$ underestimation above 60 A) actually serves a protective purpose, providing an intentional safety buffer that helps prevent stranding in areas where rescue infrastructure is limited.

Although the system demonstrated that the GPR is the best model for the electric boat deployment, the results might change in the future. The system architecture enables continuous adaptive learning through periodic model retraining. As new operational data accumulate in the cloud database, updated battery capacity parameters and discharge behavior patterns are used to retrain the regression model. These updates are automatically deployed to the electric boat through MQTT configuration messages, enabling the system to adapt to battery aging, seasonal environmental changes, and evolving operational profiles without requiring manual intervention or hardware replacement, thereby sustaining reliability and accuracy throughout the boat's operational life.

While the proposed system demonstrates high predictive accuracy ($R^2 = 0.957$), it is important to acknowledge the statistical limitations inherent in the pilot dataset. The results of the prediction stage are subject to limitations related to the dataset. Although the data are real-world measurements, they correspond to a short operational period of a single vessel. Therefore, the models' generalization capability across different vessels or operational contexts cannot be fully established. It is important to note that these data are employed exclusively for model training, as operational data from the vessel currently under development are not yet available. By leveraging data from a vessel with similar characteristics and operating conditions, the models can learn fundamental operational patterns in advance.

We trained the model on validated records collected over three days of operation, which features a temporal bias specific to the beginning of the Amazonian rainy season (*i.e.*, intense and almost daily rainfall, very high humidity, increased river levels and flooding, and milder temperatures). Consequently, the model's accuracy may fluctuate if deployed immediately in significantly different environmental conditions, such as the dry season, or under extreme load scenarios not yet encountered. To mitigate these limitations, the system architecture incorporates a continuous learning pipeline.

5 Conclusion

This article introduced an intelligent system for range estimation and trip management in electric boats, motivated by the need to improve the reliability and predictability of electric mobility in remote regions such as the Brazilian Amazon basin. The proposed system integrates real-time sensor monitoring, data pre-processing, battery discharge modeling, and ML techniques to provide accurate autonomy estimation and operational insights for river transport. From a broader perspective, this article contributes to advancing electric mobility infrastructure in regions where conventional connectivity and charging networks are scarce.

The system combines embedded sensing modules, an MQTT-based communication layer, and cloud-based visualization dashboards. This design was robust to intermittent connectivity and limited bandwidth, achieving real-time synchronization and efficient data transfer between the electric boat and the cloud platform. The modularity of the system also enables future expansion to multi-boat monitoring and distributed fleet management. These findings demonstrate the potential of integrating real-time data collection and intelligent analytics to mitigate range anxiety, optimize energy use, and promote sustainable navigation in riverine environments.

We evaluated the system using real operational data collected from the Poraquê I electric boat, where GPR achieved the best balance between predictive accuracy and computational efficiency for embedded deployment, with an R^2 of 0.957 and a MAPE of 8.307%. The battery discharge model incorporates Peukert's Law with a coefficient of $k = 1.07$ based on literature values for LiFePO4 chemistry, accounting for the nonlinear relationship between discharge current and usable capacity. These results confirm the feasibility of combining probabilistic regression and physics-based modeling to capture the nonlinear discharge characteristics of LiFePO4 maritime batteries under dynamic load conditions.

For future work, we plan to extend the system through adaptive learning mechanisms that allow online recalibration of predictive models, the incorporation of environmental variables such as temperature, current velocity, and river flow data, and the validation of scalability using the upcoming Poraquê II electric boat. An important enhancement will be the integration of SoC and SoH variables from the Battery Management System as direct input features to the ML models.

As the Poraquê I continues operation, the database will expand to cover full seasonal cycles, and the model will be periodically retrained to reduce these biases and improve long-term generalization without requiring manual intervention. Future expansions of this work are planned to incorporate additional sensing capabilities, enabling the collection of vessel load data (which influences propulsion energy demand through variations in hydrodynamic resistance) and other relevant operational and environmental variables.

Acknowledgements

This work was carried out with the support of the Coordenação de Aperfeiçoamento de Pessoal de Nível Superior – Brasil (CAPES) – Finance Code 001, the Conselho Nacional de Desenvolvimento Científico e Tecnológico (CNPq) – CNPq Fellow – Brazil (191945/2025-0), and the Fundação Amazônia de Amparo a Estudos e Pesquisas (FAPESPA). The authors also acknowledge the collaboration of Norte Energia S.A., responsible for the Belo Monte Hydroelectric Power Plant, for enabling the data collection and providing logistical support for field experiments. Special thanks are extended to the Instituto de Energia e Ambiente (IEE/UFPA) and the Poraquê Project team for their technical assistance and continued contributions to the development of sustainable electric mobility solutions in the Amazon region.

Authors' Contributions

T.A. developed and tested the prediction models and wrote the draft. J.S. conceived and developed the Operator Dashboard and helped with the draft. D.R. produced the figures and managed the referencing. M.M. implemented the Command Center Dashboard and configured the MongoDB infrastructure. L.B., I.M., E.L., D.Ro., A.A., and E.C. contributed to manuscript revision and provided critical feedback throughout the development of the work.

Competing interests

The authors declare that they have no competing interests.

Availability of data and materials

The datasets generated and/or analyzed during the current study are available in the following link: `https://drive.google.com/drive/folders/1WTBliAgrfDwRwH4g2sRQFG_qOXwXH78H?usp=sharing`.

References

Ahmed, M., Mao, Z., Zheng, Y., Chen, T., and Chen, Z. (2022). Electric vehicle range estimation using regression techniques. *World Electric Vehicle Journal*, 13(6):105. DOI: 10.3390/wevj13060105.

Al Amerl, A., Oukkacha, I., Camara, M. B., and Dakyo, B. (2021). Real-time control strategy of fuel cell and battery system for electric hybrid boat application. *Sustainability*, 13(16):8693. DOI: 10.3390/su13168693.

Candelo-Beccera, J. E., Maldonado, L. B., Sanabria, E. P., Pestana, H. V., and García, J. J. (2023). Technological alternatives for electric propulsion systems in the waterway sector. *Energies*, 16(23):7700. DOI: 10.3390/en16237700.

Chen, T. and Guestrin, C. (2016). Xgboost: A scalable tree boosting system. In *Proceedings of the 22nd acm sigkdd international conference on knowledge discovery and data mining*, pages 785–794. DOI: 10.48550/arXiv.1603.02754.

Chen, W., Tai, K., Lau, M., Abdelhakim, A., Chan, R. R., Ådnanes, A. K., and Tjahjowidodo, T. (2022). Data-driven propulsion load profile prediction for all-electric ships. In *2022 International Conference on Electrical, Computer, Communications and Mechatronics Engineering (ICECCME)*. DOI: 10.1109/ICECCME55909.2022.9988368.

Damian, S. E., Wong, L. A., Shareef, H., Ramachandaramurthy, V. K., Chan, C., Moh, T., and Tiong, M. C. (2022). Review on the challenges of hybrid propulsion system in marine transport system. *Journal of Energy Storage*, 56:105983. DOI: 10.1016/j.est.2022.105983.

De Vera, A. M. Z. and Cruz, F. R. G. (2022). Estimation of remaining travel range of electric boat using extended kalman filter. In *2022 IEEE International Power and Renewable Energy Conference (IPRECON)*, pages 1–5. DOI: 10.1109/IPRECON55716.2022.10059494.

Deng, H., Runger, G., Tuv, E., and Vladimir, M. (2013). A time series forest for classification and feature extraction. *Information Sciences*, 239:142–153. DOI: 10.48550/arXiv.1302.2277.

Dos-Reis, M., Frison, C. I., Teixeira, F. C., and Marques-Neto, H. T. (2024). Using electric vehicle driver's driving mode for trip planning and routing. *Journal of Internet Services and Applications*, 15(1):410–423. DOI: 10.5753/jisa.2024.3805.

Friedman, J. H. (2001). Greedy function approximation: a gradient boosting machine. *Annals of statistics*, pages 1189–1232. DOI: 10.1214/aos/1013203451.

Galushkin, N. E., Yazvinskaya, N. N., and Galushkin, D. N. (2020). A critical study of using the peukert equation and its generalizations for determining the remaining capacity of lithium-ion batteries. *Applied Sciences*, 10(16):5518. DOI: 10.3390/app10165518.

Hernández-Fontes, J. V., Maia, H. W. S., Chávez, V., and Silva, R. (2021). Toward more sustainable river transportation in remote regions of the amazon, brazil. *Applied Sciences*, 11(5):2077. DOI: 10.3390/app11052077.

Hosseini, S., Yassine, A., and Akilan, T. (2024). Ensemble-based robust model for accurate driving range estimation of evs leveraging big data. In *2024 IEEE 8th Energy Conference (ENERGYCON)*, pages 1–6. IEEE. DOI: 10.1109/ENERGYCON58629.2024.10488792.

Intelligence, M. (2025). Electric boat and ship market – growth, trends and forecast (2025-2030). Available at:`https://www.mordorintelligence.com/industry-reports/electric-boat-and-ship-market`. accessed 2025-10-20.

Jung, S., Jeong, S., Kang, J., and Kang, J. (2023). Marine iot systems with space-air-sea integrated networks: Hybrid leo and uav edge computing. DOI: 10.48550/ARXIV.2301.03815.

Kersey, J., Popovich, N. D., and Phadke, A. A. (2022). Rapid battery cost declines accelerate the prospects of all-electric interregional container shipping. *Nature Energy*, 7(7):664–674. DOI: 10.1038/s41560-022-01065-y.

Kistner, L., Bensmann, A., and Hanke-Rauschenbach, R. (2023). Potentials and limitations of battery-electric container ship propulsion systems. *Journal Name*. DOI: 10.15488/16850.

Li, X., Chang, H., Wei, R., Huang, S., Chen, S., He, Z., and Ouyang, D. (2023). Online prediction of electric vehicle battery failure using lstm network. *Energies*, 16(12):4733. DOI: 10.3390/en16124733.

Lima, F. C. d. L., Rodrigues, I. C. d. S., Pompeu, L. L., Sousa, A. R. M. d., Fonseca, W. d. S., and Silva, M. d. O. e. (2024). The challenges of naval electromobility in amazônia. *Revista de Gestão Social e Ambiental*, 18(7):e07778. DOI: 10.24857/rgsa.v18n7-194.

Lobato, E., Prazeres, L., Medeiros, I., Araújo, F., Rosário, D., Cerqueira, E., Tostes, M., Bezerra, U., Fonseca, W., and Antloga, A. (2022). A monitoring system for electric vehicle charging stations: A prototype in the amazon. *Energies*, 16(1):152. DOI: 10.3390/en16010152.

Malheiros, G. (2023). Inland waterborne transportation sets new record in brazil's 3q23. Available at:`https://datamarnews.com/noticias/inland-waterborne-transportation-sets-new-record-in-brazils-3q23/`. Accessed: 2025-10-20.

Martins, J. A. and Rodrigues, J. M. F. (2025). Intelligent monitoring systems for electric vehicle charging. *Applied Sciences*, page 2741. DOI: 10.3390/app15052741.

Mazzei, M. (2024). Primeira voadeira elétrica da região amazônica faz viagem inaugural no xingu. Available at: `https://www.norteenergiasa.com.br/noticias/primeira-voadeira-eletrica-da-regiao-amazonica-faz-viagem-inaugural-no-xingu-1351`. Accessed: 2025-09-26.

Moon, H. S., Park, W. Y., Hendrickson, T., Phadke, A., and Popovich, N. (2024). Exploring the cost and emissions impacts, feasibility and scalability of battery electric ships. *Nature Energy*, 10(1):41–54. DOI: 10.1038/s41560-024-01655-y.

Norte Energia (2023). Belo monte: Gigante por natureza. Available at: `https://www.norteenergiasa.com.br/uhe-belo-monte/`. Accessed: 2025-09-27.

Oyediran, D., Thakur, J., Khalid, M., and Baskar, A. G. (2024). Electrification of marinas in stockholm: Optimizing charging infrastructure for electric boats. *Energy*, 305:132311. DOI: 10.1016/j.energy.2024.132311.

Pokharel, S., Sah, P., and Ganta, D. (2021). Improved prediction of total energy consumption and feature analysis in electric vehicles using machine learning and shapley additive explanations method. *World Electric Vehicle Journal*, 12(3):94. DOI: 10.3390/wevj12030094.

Rudy, A. S., Skundin, A. M., Mironenko, A. A., and Naumov, V. V. (2023). Current effect on the performances of all-solid-state lithium-ion batteries—peukert's law. *Batteries*, 9(7):370. DOI: 10.3390/batteries9070370.

Saqr, A. E.-S., Saraya, M. S., and El-Kenawy, E.-S. M. (2025). Enhancing co2 emissions prediction for electric vehicles using greylag goose optimization and machine learning. *Scientific Reports*, 15(1):16612. DOI: 10.1038/s41598-025-99472-0.

Simavari, P., Pazouki, K., and Norman, R. (2025). Decarbonising the inland waterways: A review of fuel-agnostic energy provision and the infrastructure challenges. *Energies*, 18(19):5146. DOI: 10.3390/en18195146.

Smola, A. J. and Schölkopf, B. (2004). A tutorial on support vector regression. *Statistics and computing*, 14(3):199–222. DOI: 10.1023/B:STCO.0000035301.49549.88.

Sulaiman, M. H. and Mustaffa, Z. (2024). State of charge estimation for electric vehicles using random forest. *Green Energy and Intelligent Transportation*, 3(5):100177. DOI: 10.1016/j.geits.2024.100177.

Yazvinskaya, N. N., Galushkin, N. E., Ruslyakov, D. V., and Galushkin, D. N. (2021). Analysis of peukert and liebenow equations use for evaluation of capacity released by lithium-ion batteries. *Processes*, 9(10):1753. DOI: 10.3390/pr9101753.

Zeng, A., Ho, H., and Yu, Y. (2020). Prediction of building electricity usage using gaussian process regression. *Journal of Building Engineering*, 28:101054. DOI: 10.1016/j.jobe.2019.101054.

Zhao, L., Yao, W., Wang, Y., and Hu, J. (2020). Machine learning-based method for remaining range prediction of electric vehicles. *IEEE Access*. DOI: 10.1109/ACCESS.2020.3039815.

Zhou, L., Yao, G., Wang, H., Li, J., Liu, S., and Nie, Y. (2024). *Research on Integrated Energy Management Strategy of Ships Based on Internet of Things Technology*, pages 12–22. IOS Press. DOI: 10.3233/atde231086.